Supplementary Information (SI) for Nanoscale Horizons.
This journal is © The Royal Society of Chemistry 2025

Supplementary

Phase-Change Wax Integrated with Rapid Carbon Nanotube Array for Spatial Light Modulation

*Liwen Lai,[a,b] Peng Liu,[*b] Chunhai Zhang,[b] Duanliang Zhou,[b] Qunqing Li[**b] and Shoushan Fan[b]*

[a.]Tsinghua Shenzhen International Graduate School, Tsinghua University, Shenzhen 518055, China

[b.]Department of Physics, State Key Laboratory of Low-Dimensional Quantum Physics & Tsinghua-Foxconn Nanotechnology Research Center, Tsinghua University, Beijing 100084, China

*Corresponding author. E-mail: pengliu@tsinghua.edu.cn qunqli@tsinghua.edu.cn

High transmittance glass substrate insensitive to wavelength.

To achieve significant light flux transmission, a transparent substrate was selected for the experiment. Sodium calcium glass, known for its high transmittance across the visible to near-infrared spectrum, was chosen as the substrate for screen printing. The sodium calcium glass used in the experiment had a thickness of 0.33 μm and exhibited transmittance above 90% across the entire range of 350–1100 nm, as depicted in Fig. S1. The transmittance spectrum remained relatively flat throughout the entire tested region, indicating that the substrate's influence on different wavelengths can be considered negligible.

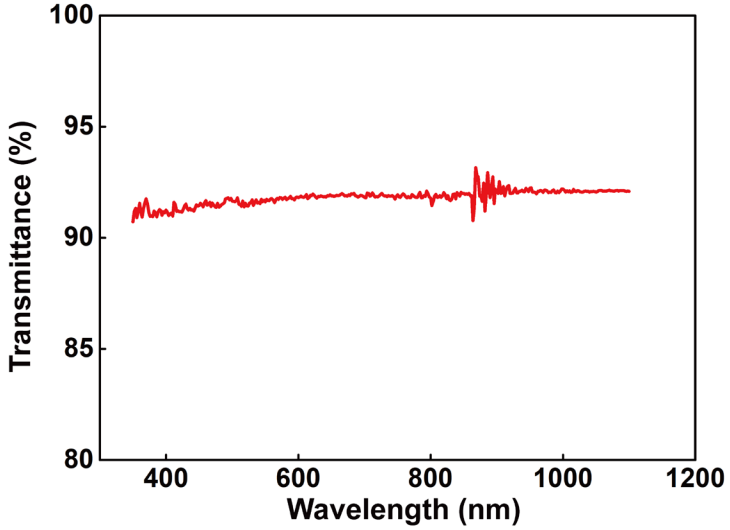

Fig. S1 Transmittance spectrum of sodium calcium glass substrate.

Fabrication method for SACNT film heater array.

The fabrication method for SACNT film heater arrays via screen printing involves an eight-step process: (1) Printing horizontal electrodes; (2) Printing insulation layers; (3) Printing vertical electrodes; (4) Printing CNT electrodes: Specific electrodes were printed to support the SACNT films, referred to as CNT electrodes.; (5) Printing adhesive electrodes: These electrodes were designed to bond the SACNT films in place, known as adhesive electrodes; (6) Laying a single layer SACNT film; (7) Laser cutting; (8) Erasing ineffective SACNT films: Finally, any non-conductive or ineffective SACNT films were removed using anhydrous ethanol to ensure purity and efficiency. Figure S2 shows all the processes diagram for preparing SACNT film arrays. In Fig. S2 (a) to S2 (h), the horizontal silver electrodes, vertical silver electrodes and CNT

electrodes are marked with dark gray, the insulating dielectric layer is marked with orange, while the adhesive electrodes are represented by white. The single-layer SACNT film is depicted by a series of parallel black lines. Both the horizontal and vertical electrodes, as well as the CNT electrodes, are conductive electrodes printed using the same silver paste. After completing each of the first four steps, the samples must be sintered and solidified at 570°C to securely attach these printed layers to the glass substrate. To firmly place the single-layer SACNT film onto the printed electrode array, a conductive adhesive layer, identical in shape, material, and position to the CNT electrode, is printed atop the CNT electrode before the SACNT film is laid down. This conductive adhesive layer is referred to as the adhesive electrode. After printing the adhesive electrodes, an SACNT film that can cover the entire array area must be layered immediately. This is followed by heating the sample on a hot plate at 150°C for 5 minutes to cure the adhesive layer and effectively bond the SACNT film to the CNT electrode. Subsequently, an ablation program is set up according to the actual size and layout of the printed array, utilizing laser cutting to precisely remove the SACNT film outside the CNT electrodes. Finally, the ineffective SACNT film is wiped off with a fine cotton swab, preserving the SACNT film between the CNT electrodes. This process results in the fabrication of a complete SACNT film array. A 16 × 16 SACNT film array was fabricated through screen printing, and the optical photograph of the entire SACNT film array is shown in Fig. S3, with a ruler for scale, measuring 6 mm in length in this photograph.

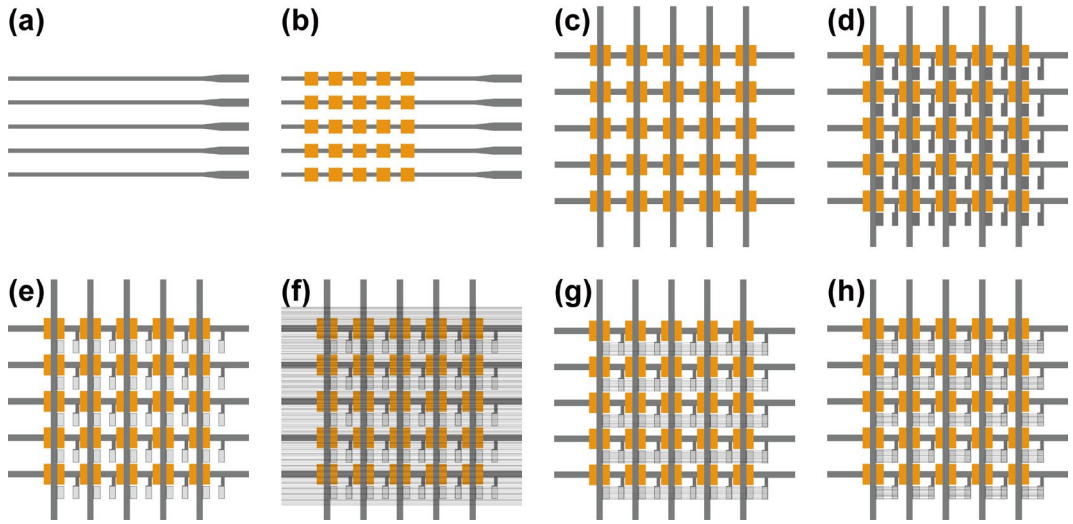

Fig. S2 Schematic diagram of SACNT film array fabrication process. (a) Printing horizontal silver electrodes; (b) Printing insulation dielectric layer; (c) Printing vertical silver electrodes; (d) Printing

CNT electrodes; (e) Printing adhesive electrodes; (f) Laying single-layer SACNT film; (g) Laser cutting; (h) Erasing ineffective SACNT films.

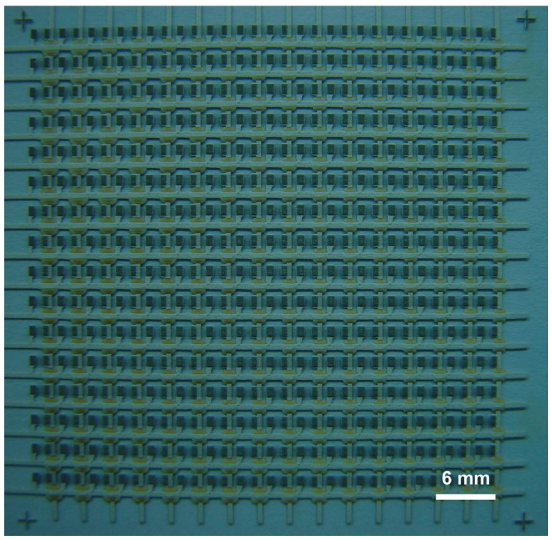

Fig. S3 The optical photograph of the entire 16 × 16 SACNT film array.

Fabrication method for the SACNT–paraffin wax composite structure.

The paraffin wax used in the experiment is a fully refined 58–particle paraffin wax, with a melting point of 58 ℃. Given that the paraffin wax particles can compress, deform, or even break the SACNT films, it is essential to apply the melted paraffin wax onto the SACNT film array. Firstly, the prepared SACNT film array and solid paraffin wax particles were placed on a hot plate, with the temperature of the hot plate maintained above the melting point of the paraffin wax. In the experiment, the temperature of the hot plate was fixed at 100°C. To prevent the wax from spreading out from the SACNT film array, a square hollow acrylic frame was affixed around the entire 16 × 16 SACNT array. After the paraffin wax had melted, it was poured along the edge of the prepared SACNT film array, and the entire substrate was then allowed to stand and cool. Once the paraffin wax had completely solidified and the substrate had cooled to room temperature, the final SACNT-paraffin wax composite structure array was obtained. The area covered by the paraffin wax on the substrate was large enough to confirm that the paraffin wax uniformly covered all the SACNT film pixels. Fig. S4

displays an image of the well-formed SACNT-paraffin wax composite structure array, with a surface density of paraffin wax of $2.23 \times 10^{-4} g/mm^2$.

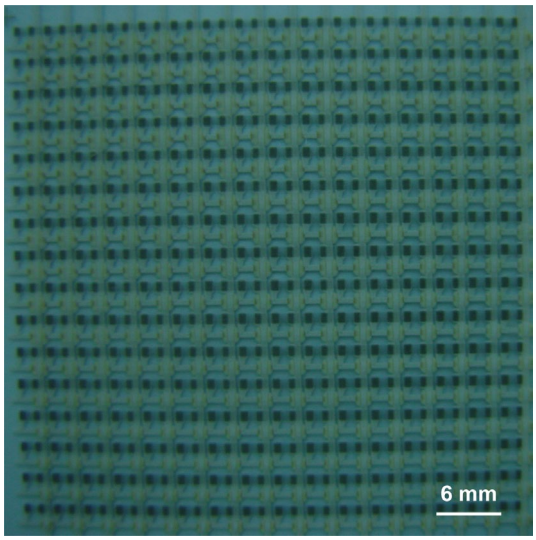

Fig. S4 The optical photograph of the 16 × 16 SACNT–paraffin wax composite structure. The surface density of paraffin wax is $2.23 \times 10^{-4} g/mm^2$.

Observation of paraffin wax melting and solidification processes.

Subsequently, a microscope equipped with a micro area spectrometer was utilized to monitor the phase change occurring on a single pixel of the SACNT-paraffin wax composite array through controlled electric heating. Throughout the entire phase transition process, 12 images of different melting and solidification stages were captured from recorded video clips. The images depicting the melting process are presented in Fig. S5, while those illustrating the solidification process are displayed in Fig. S6

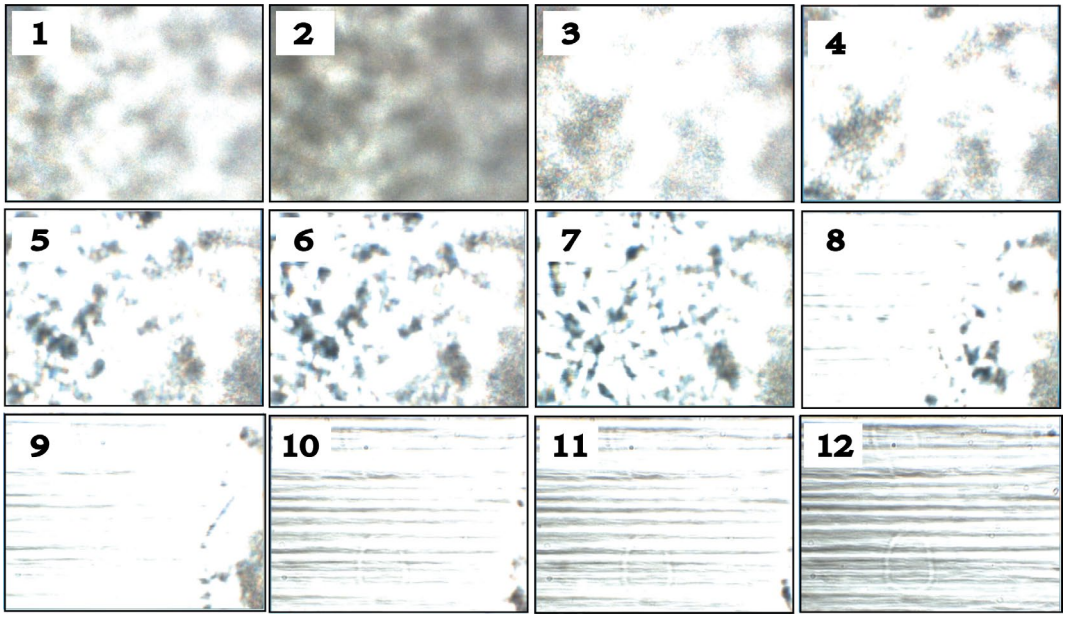

Fig. S5 Images of 12 different stages of paraffin wax melting process obtained with micro area spectrometer.

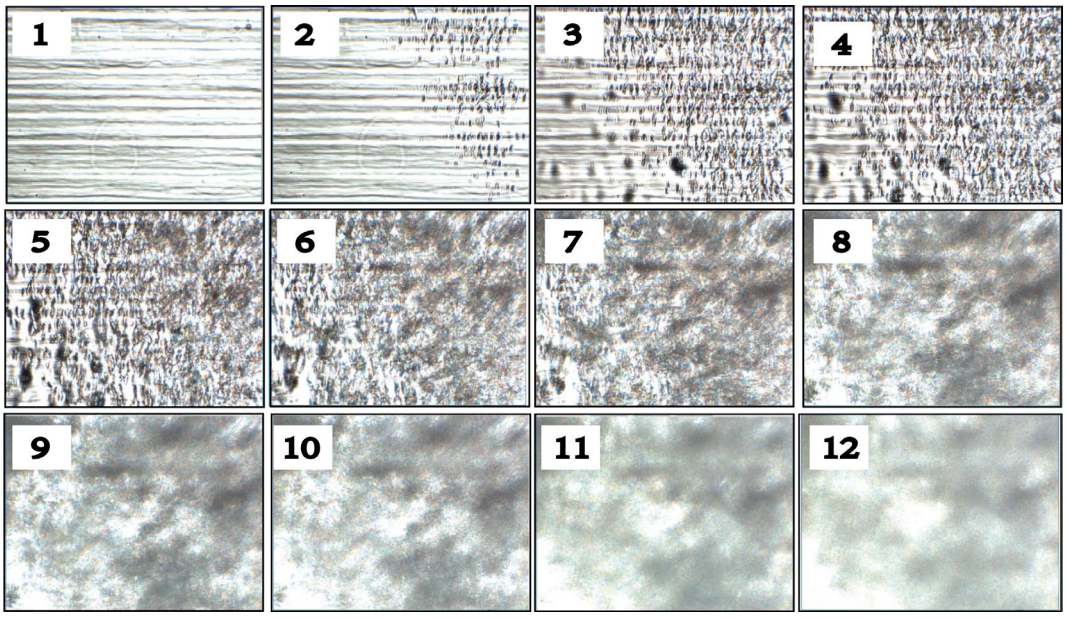

Fig. S6 Images of 12 different stages of paraffin wax solidifying process obtained with micro area spectrometer.

The direction of melting and solidification of the paraffin wax during the phase transition processes, as depicted in Fig. S5 and Fig. S6, is opposite. This observation suggests that the paraffin wax on the left side was preheated, indicating that the SACNT-paraffin wax composite array pixels on the left side reached a higher temperature compared to those on the right side. This temperature gradient implied that

the paraffin wax layer on the left side was thinner than on the right, possibly due to the sample stage not being perfectly flat. The thinner layer on the left side heated up more quickly to its melting point, initiating the melting process starts from that side. Similarly, in Fig. S6, the solidification of paraffin wax progressed from right to left, indicating that the temperature on the right side was lower than that on the left. Consequently, when the power was cut off, the paraffin wax on the right side began to crystallize and solidify first. Additionally, in Fig. S6, the paraffin wax adjacent to the SACNT film solidified before that further away. This was attributed to the SACNT film having a lower heat capacity than that of the paraffin wax, causing its temperature to drop more rapidly after the power being turned off. As a result, the paraffin wax near the SACNT film cooled more quickly, affecting both the solidification and melting processes.

Optical picture of periodic electric heating composite structure array and the numbering of rows and columns in the array.

The density of paraffin wax of the periodic electric heating composite structure array is $1.17 \times 10^{-4} g/mm^2$. To prevent damage to the SACNT-paraffin wax composite structure, acrylic frames were used to encase the entire array. Subsequently, the paraffin wax on the row and column electrodes was cleaned, and periodic electric heating was applied to one of the grid points within the composite array. The sample was suspended to facilitate the passage of light through the back of the grid points, which simplifies the observation of light shadow and transmitted signal variations and prevents additional thermal stress on the sample. The optical images of the periodic electric heating composite structure array, along with the row and column numbering, are displayed in Fig. S7(a) and (b). In Fig. S7(b), the (9,9) grid point was selected as the center for the targeted heating study.

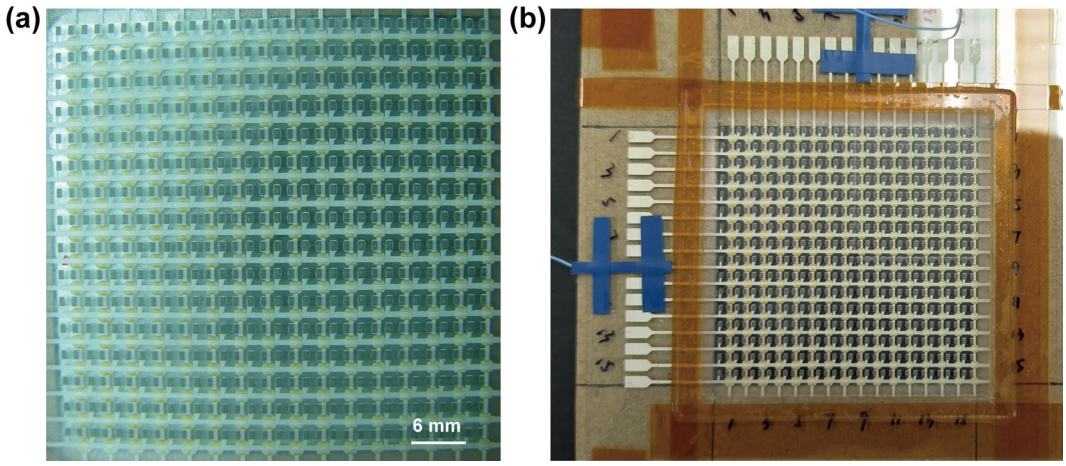

Fig. S7 (a) The optical image of periodic electric heating composite structure array. (b) The grid point numbering of rows and columns in the array.

Rough determination of appropriate heating time and pulse duty cycle.

After initial exploration, video recording was employed to identify and determine the time nodes at which the paraffin wax on the heating grid point melted and solidified. It was observed that when a direct current voltage of 6V was applied, the paraffin wax could be rapidly heated and melted, with a measured current of 0.0568 A. The (9,9) grid point was then manually powered on and off, and a video capturing the repeated melting and solidification cycles was recorded. During data processing, each second of video was divided into 30 frames. From this video, the time required for the paraffin wax to melt and solidify on the (9,9) grid point was estimated. Fig. S8 displays the captured frame images, the notation '23s 9f' in the figure refers to the 9th frame at the 23rd second, and so on. It was calculated that the melting time of the paraffin wax was approximately 17 frames, equivalent to 0.567 seconds, and the solidification time was also approximately 14 frames, equivalent to 0.467 seconds. Consequently, the total state change time for one cycle of paraffin wax melting and solidification on the (9,9) grid point at a voltage of 6V is about 1.037 seconds, and the time duty cycle for paraffin wax melting, i.e., the power on time, is 54.84%, which is approximately 55%.

It should be noted that the melting and solidification times of paraffin wax can vary significantly depending on the surface density of the paraffin wax, as well as the applied voltage and pulse duty cycle. Consequently, when a new sample is introduced, it is necessary to re-evaluate and adjust these parameters. However, once optimized for a

particular sample, these settings can serve as a reference for guiding subsequent experiments on the same sample.

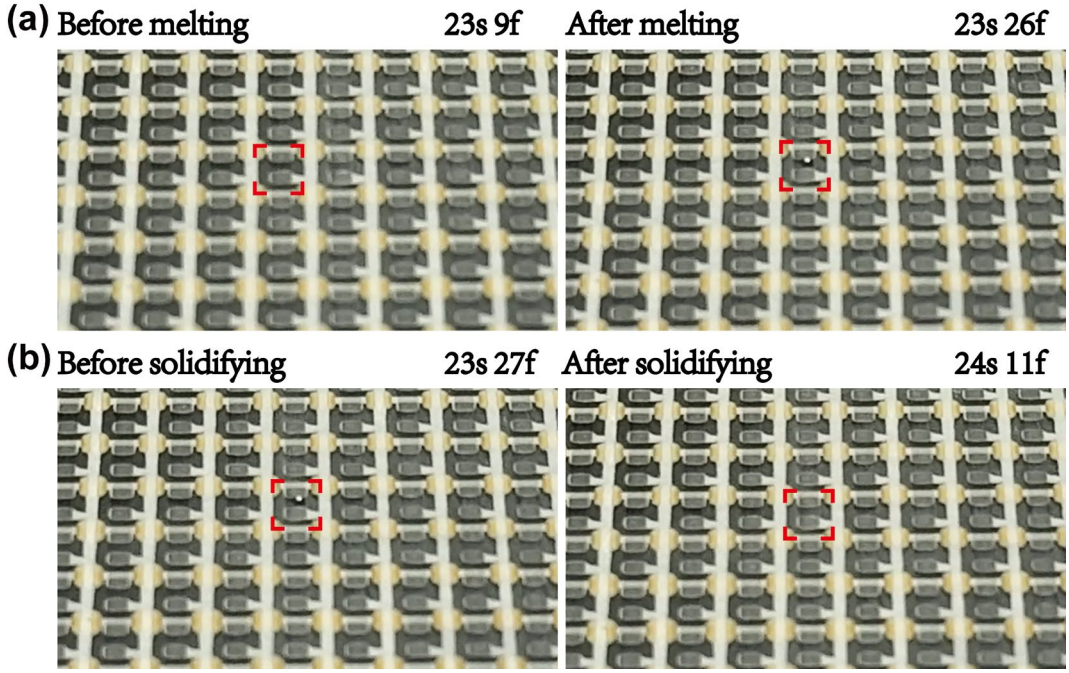

Fig. S8 Repeated electric heating images capturing the paraffin wax undergoing melting and solidification at the (9,9) grid point. The phase transitions of the paraffin wax at this point are recorded as two distinct processes: (a) Melting process; (b) Solidification process.

Repeated heating leads results in thinning of paraffin wax at the grid points.

It's important to note that since the paraffin wax on each grid point is not isolated, the repeated melting and solidification of the wax at a single grid point leads to thinning at that location. Fig. S8 displays an image of a grid point after multiple heating cycles, where it is evident that the paraffin wax has formed protrusions on both sides with a more transparent pit in the center, indicating a decrease in the density of the paraffin wax at that grid point. When the paraffin wax at this point melts, it gains fluidity, and surface tension causes the wax to flow and extend towards the edge. The temperature at the edge is lower and closer to the ambient temperature, which is insufficient for the paraffin wax to melt under brief electric heating. Consequently, the paraffin wax that extends to the edge solidifies, resulting in a reduction of paraffin wax at the heating center and further thinning at that grid point. Therefore, after several heating cycles, the

paraffin wax at the edges of the SACNT film array within the grid will gradually become thicker.

Due to the thinning of paraffin wax at a specific grid point caused by repeated electric heating, this point is no longer suitable for further electrical modulation experiments. It is recommended to select another grid point for such tests. For future work, an improved method could involve printing insulation patterns with closed hollow contours on each grid, ensuring the pattern being larger than the contour size of each SACNT film between CNT electrodes. This would help to maintain a consistent amount of paraffin wax on the grid. Fig. S9 shows optical images of the (9,9) grid point, marked with a red dashed box, where the paraffin wax has become thinner due to repeated electric heating. The electrical crosstalk issue in the passive addressing circuitry has also caused noticeable current dividers at the four points near the grid point, leading to thinning of the paraffin wax at these locations as well. To mitigate the risk of heat accumulation and significant wax thinning over extended heating periods, it is suggested that smaller duty cycle pulses be used in subsequent periodic heating experiments.

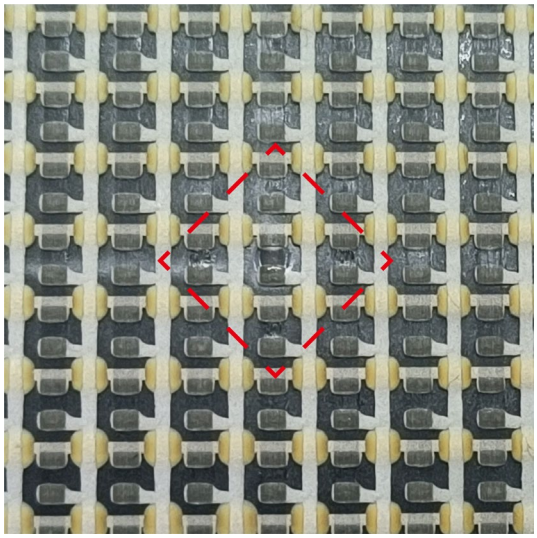

Fig. S9 Repeated electric heating causes the paraffin wax on the (9,9) grid point marked with a red dashed box becoming thinner.